NMR and NQR study of atomic motion below 500 K in $YBa_2Cu_3O_7$

Susan P. Klein*
Department of Physics, Oregon State University, Corvallis, Oregon 97331-6507

Rui-Ping Wang† and Arthur W. Sleight
Department of Chemistry, Oregon State University, Corvallis, Oregon 97331-4003

William W. Warren, Jr.
Department of Physics, Oregon State University, Corvallis, Oregon 97331-6507
(Received 26 December 1996)

Measurements of the intensity of the ^{63}Cu NQR and quadrupolar-satellite NMR at elevated temperatures are reported for the planar Cu(2) sites in samples of nominal composition $YBa_2Cu_3O_7$. It is observed that spin-echo intensities decrease dramatically between room temperature and 500 K and that the onset of intensity loss occurs at lower temperatures in more defective samples. Measurements of the spin-echo decay rates reveal that the intensity loss is associated with loss of phase coherence exceeding that expected from spin-spin and spin-lattice relaxation. By means of a simple, illustrative model, these effects can be attributed to changes in the local atomic environment, presumed to be caused by motion of oxygen atoms in the Cu(1) layer. These motions occur on a time scale on the order of 10 μs at 500 K and their probability is enhanced at lower temperatures by the presence of structural defects. [S0163-1829(97)00733-9]

I. INTRODUCTION

It is well known that the concentration and structural arrangement of oxygen plays a crucial role in the high-temperature superconductor $YBa_2Cu_3O_{6+x}$. Oxygen is the dopant which controls the carrier (hole) concentration and yields optimally doped material with a 93 K superconducting transition temperature T_c for values of x very close to 1.0. The now familiar layered structure of this material is based on CuO_2 planes and a layer containing CuO chains. In underdoped material, T_c depends strongly on oxygen content and is affected by the structure of a variety of ordered arrangements of oxygen in the chain layer.

A number of recent studies have shown that oxygen is unexpectedly mobile near, and even below, room temperature. These motions can produce significant changes in material properties within a few hours or even less, depending on the temperature. Veal *et al.*,[1,2] observed that the superconducting transition temperature increased with time as quenched underdoped samples were annealed at temperatures between 273 and 423 K. The time required to reach an apparent steady state at room temperature was roughly 10 h. In their neutron-diffraction studies of $YBa_2Cu_3O_{6.41}$, Jorgenson *et al.*[3] observed changes of T_c and various bond lengths on the scale of a few hours. Hadjiev *et al.*[4] reported similar room-temperature annealing effects on the Raman spectra of underdoped single crystals ($x \approx 6.5$).

These effects have generally been attributed to the ordering of oxygen in the layer containing CuO chains. The chains, formed by alternate sites denoted Cu(1) and O(1), are separated by oxygen sites O(5) which are all unoccupied in the ideal $YBa_2Cu_3O_7$ structure. The possible oxygen sites in this layer O(1) and O(5) thus form a nearly square lattice on which oxygen is ordered in at least two ways. The first type of order is the preferential occupation of O(1) sites with depletion of O(5) sites to form Cu(1)-O(1) chains in the ideal $YBa_2Cu_3O_7$ structure. The second form of order occurs in underdoped material ($x<1$) in which O(1) vacancies cluster in ''empty chains'' so as to maximize the length of intact chain segments. Ordered structures based on alternating ''full'' and ''empty'' chains have been proposed.[5] A number of authors[5–8] have pointed out that by increasing the number of twofold coordinated Cu(1) sites with electronic configuration Cu^+, formation of ''empty chains'' can enhance T_c by increasing the hole concentration in the CuO_2 planes.

In the neutron-diffraction studies,[3] essentially no change was found in the occupation of O(5) and O(1) sites as T_c and bond lengths relaxed after quenching. This suggests that chain ordering [rearrangement of occupied O(1) sites] rather than chain *formation* [movement of oxygen from O(5) to O(1)] is responsible for the annealing effects. Numerical simulations[8] support this idea and yield two time constants differing by an order of magnitude for formation of chain-ordered phases in underdoped material. The shorter time ($\sim$100 min at room temperature) was associated with the O(5)$\rightarrow$O(1) chain formation process.

Nuclear magnetic resonance (NMR) and nuclear quadrupole resonance (NQR) can be extremely sensitive to atomic motion on the scale of interatomic distances. The resonance properties of nuclei with nuclear quadrupole moments, such as ^{63}Cu and ^{65}Cu, are profoundly affected by the local electric field gradient (EFG) determined by the arrangement of electronic and nuclear charge around a particular class of crystalline site. In the case of NQR, the resonance frequency is directly proportional to the local EFG whereas in NMR the electric quadrupole interaction is a perturbation which introduces splittings and broadening to the spectrum. These effects are so strong that it is possible to distinguish features of the NMR and NQR spectra associated with specific types of crystalline sites, such as the Cu(1) chain and Cu(2) plane

sites. The sensitivity of NQR to local structure in $YBa_2Cu_3O_{6+x}$ is such that distinct lines can even be resolved for various oxygen-ordered structures in underdoped material.[7,9,10] In nominal optimally doped stoichiometric $YBa_2Cu_3O_7$, the presence of defects and lattice strains can broaden and distort the NQR line shape. Given this high sensitivity to local structure, it is not surprising that NMR and NQR spectra are affected by short-range atomic motions if they occur on an appropriate time scale.

The present study was motivated by the observation of dramatic losses of NQR spin-echo intensities in nominal $YBa_2Cu_3O_7$ at relatively low elevated temperatures, i.e., between room temperature and about 500 K. We are, in fact, aware of no NQR data reported for sample temperatures above 500 K.[11] In contrast, ^{63}Cu NQR data for the double-chain compound $YBa_2Cu_4O_8$ have been reported for temperatures up to 800 K.[12] Given the relatively stable structure of $YBa_2Cu_4O_8$ in contrast with the high concentration of empty O(5) sites and evidence of oxygen motion in $YBa_2Cu_3O_{6+x}$, it is natural to suspect that the NQR anomalies in $YBa_2Cu_3O_7$ are related to low-temperature motion of oxygen. In this paper we report a study of the temperature-dependent NQR and NMR intensities in samples of nominal composition $YBa_2Cu_3O_7$ in order to determine the time scale of the relevant motions and their relation to defects.

II. EXPERIMENTAL DETAILS

$YBa_2Cu_3O_7$ samples were prepared by solid-state reaction of the oxides Y_2O_3, $BaCO_3$, and CuO. The powders were ground together, compressed into pellets, and heated at 850 °C in air for 16 h. The powder was then reground and heated at 950 °C in air for 16 h. This step was repeated. Finally, the powder was ground, compressed again, and heated in O_2 for 48 h. This was followed by a slow cool to 25 °C at 1°/min under O_2. X-ray-diffraction measurements showed that the samples were single-phase $YBa_2Cu_3O_7$. The superconducting transition temperatures of these samples were determined to be 92 K by ac susceptibility measurements. To eliminate radio-frequency skin depth effects, the pellets were reduced to powder for NMR and NQR studies. Finally, the samples were sealed in Pyrex or quartz tubes containing 0.5–1.0 atm of oxygen in order to provide long-term stability over the course of the experiments.

NQR data were obtained by standard ($\pi/2$-τ-π) spin-echo sequences using a home-built coherent pulsed NMR spectrometer. A home-built high-temperature probe provided elevated sample temperatures using a heated air flow. This spectrometer does not have full phase-cycling capability so spurious ringing signals were suppressed in the NQR measurements by alternately adding and subtracting signals obtained with τ values of 25 and 40 μs, respectively.[13] NQR spectra were obtained by plotting the integral of the echoes versus the applied radio frequency.

Similar techniques were used to obtain NMR spectra in an 8.0 T magnetic field. A Chemagnetics/Otsuka CMX-340 spectrometer provided pulse sequences with full phase cycling and a heated air flow for variable sample temperatures. The NMR spin-echo τ value was typically 20 μs.

III. EXPERIMENTAL RESULTS

A. NQR spectra at room temperature

The frequency of an NQR transition is uniquely determined by the local atomic arrangement. Thus the NQR intensity and linewidth are extremely sensitive to the presence of crystalline defects. A lattice site next to a vacancy, for example, can be expected to exhibit an NQR frequency so different from that of sites with standard coordination that such a highly defective site will not contribute at all to the NQR line of the standard sites. More subtle or more distant defects, on the other hand, introduce local strains and small NQR shifts which broaden the NQR line.

The shape and width of the planar Cu(2) NQR line in nominal $YBa_2Cu_3O_7$ are dramatically affected by small changes in oxygen content. In a systematic study of linewidth versus oxygen deficiency, Schiefer *et al.*[14] observed an increase in linewidth ($\Delta\nu \equiv$ full width at half maximum) from 200 to 300 kHz as the deficiency increased from 2 to 4 %, i.e., as x decreased from 0.98 to 0.96 according to their oxygen determination. Because oxygen vacancies are introduced mainly in the chain layer with decreasing x, this inhomogeneous broadening reflects distortions of the atomic positions and electronic charge distribution in response to the chain layer vacancies.

The room temperature Cu(2) NQR lines of two of the samples used in this study are shown in Fig. 1. The ''better'' sample (A) has a linewidth $\Delta\nu = 225$ kHz. Such a sample would correspond to $YBa_2Cu_3O_{6.98}$ on the oxygen scale used by Schiefer *et al*. We cannot, however, exclude the possibility that other defects such as cation disorder contribute to the observed broadening. The resonance of the second, and ''poorer'' sample (B) shown in Fig. 1 has a linewidth $\Delta\nu \approx 300$ kHz and a pronounced shoulder on the low-frequency side of the line. The appearance of additional Cu(2) NQR lines at lower frequencies is a characteristic of oxygen-deficient material.[7,9,10] An x-ray microprobe examination of this sample revealed small variations of oxygen content within a single grain. The Cu(1) NQR lines of both samples exhibited low-frequency shoulders. However, despite the dramatic differences in their Cu(2) NQR lines, both samples yielded sharp superconducting transitions and ''ideal'' $YBa_2Cu_3O_7$ x-ray patterns.

B. NQR spectra at elevated temperatures

The Cu(2) NQR spin-echo spectrum of sample A is shown in Fig. 2 at a series of temperatures up to 450 K. With increasing temperature, the resonance shifted to lower frequency and lost intensity at fixed τ values *without a significant change in linewidth*. The temperature-dependent frequency shift is consistent with previous data[15] obtained at temperatures below room temperature (Fig. 3). The temperature-dependent frequency shift can be generally attributed to the effects of thermal expansion on the various contributions to the EFG at the Cu sites.

The observed behavior of NQR intensity with increasing temperature is anomalous. For given pulse conditions and constant nuclear spin-spin and spin-lattice relaxation times, the spin-echo intensity should be proportional to the nuclear polarization, i.e., the intensity should vary inversely as the absolute temperature (Curie law). To compare the observed

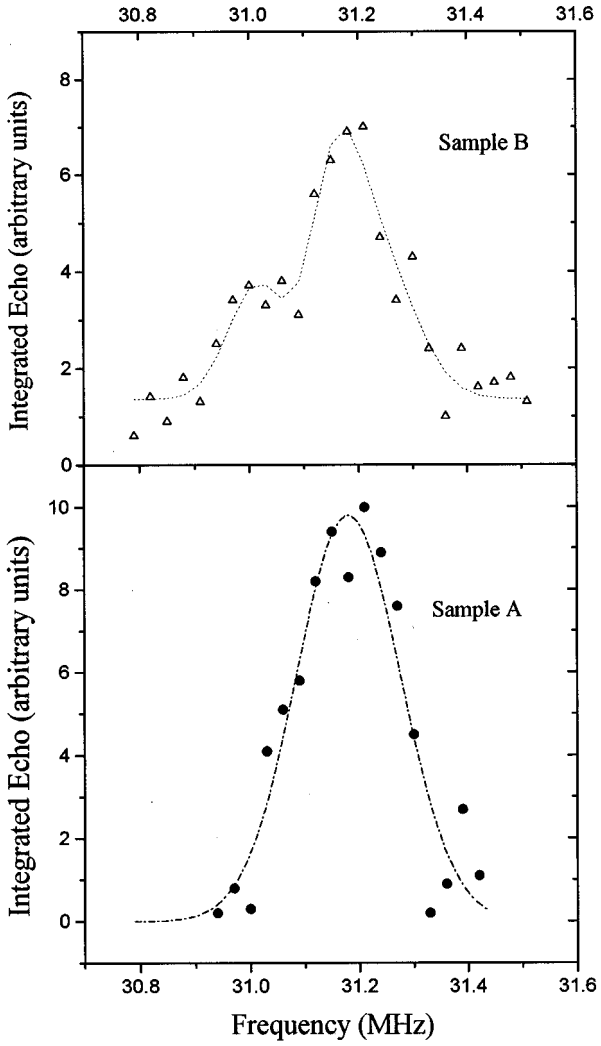

FIG. 1. Room-temperature ^{63}Cu(2) NQR spin-echo spectra of sample A (lower panel) and sample B (upper panel).

intensities with this behavior we plot in Fig. 4 the integrated NQR spin-echo intensity times temperature ($I\times T$). This quantity should be independent of temperature in the ideal case. It can be seen that for sample A, ($I\times T$) is roughly constant up to about 400 K, then decreases rapidly to nearly zero at 475 K. We were unable to observe an NQR signal from this sample at 500 K. This effect was found to be fully reversible in this sample with full recovery of the NQR intensity when the sample was returned to room temperature. As we discuss in more detail later, this loss of spin-echo intensity cannot be explained by the ordinary effects of spin-spin and spin-lattice relaxation. We observed a similar loss of intensity for the Cu(1) NQR line, although the decrease occurred over a somewhat wider range of temperature. Again, in this case, no Cu(1) NQR signal was observable at 500 K. Given the qualitatively similar behavior of Cu(1) and Cu(2), we have emphasized the behavior of the Cu(2) NQR intensities in this study so as to avoid interpretive complications introduced by the strongly temperature-dependent spin-lattice relaxation rate of Cu(1).[11] In contrast, the relaxation rate of Cu(2) is nearly independent of temperature in the experimental range. To assure that these intensity losses were not due to a decrease in probe sensitivity at elevated

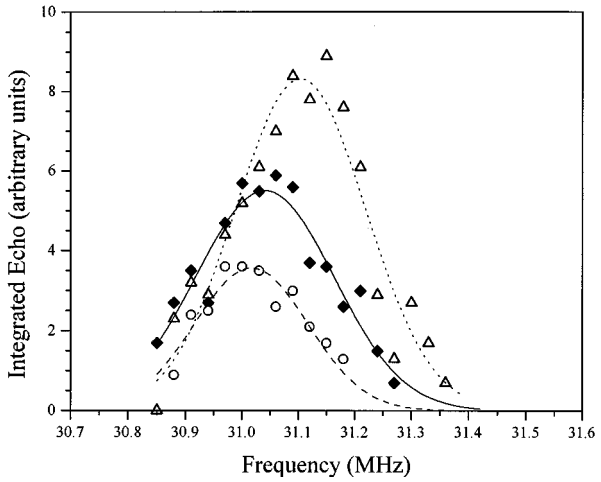

FIG. 2. ^{63}Cu(2) NQR spin-echo spectra of sample A at 350 K (open triangles), 425 K (closed diamonds), and 450 K (open circles). The pulse delays in the spin-echo sequences were maintained at constant τ values of 25 and 40 μs as the temperature was varied.

temperatures, the spectrometer was calibrated using the 26 MHz ^{63}Cu NQR signal from Cu_2O. The intensity $I\times T$ of this signal was observed to be constant over the range 300–500 K.

The temperature dependence of NQR intensity was found to be sample dependent. After a first heating to 500 K, the room-temperature spin-echo intensity of the more defective sample B was irreversibly reduced by about 30%. The variation of intensity during subsequent heatings, however, was fully reversible and reproducible. This behavior, shown in Fig. 4, exhibits a uniform decrease in $I\times T$ from room temperature to 425 K at which point the signal had essentially disappeared. By comparison, the temperature-corrected intensity of sample A was only slightly reduced from its room-temperature value at this temperature. When sample B was cooled *below* room temperature, we found that the intensity only obeyed the Curie law at temperatures below about 225 K.

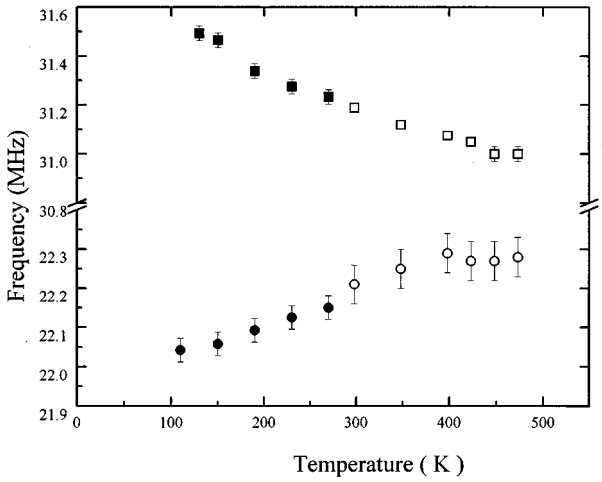

FIG. 3. ^{63}Cu NQR frequency versus temperature for Cu(1) (circles) and Cu(2) (squares). Data for temperatures below room temperature, denoted by closed points are quoted from Ref. 15; open points denote present data obtained at elevated temperatures.

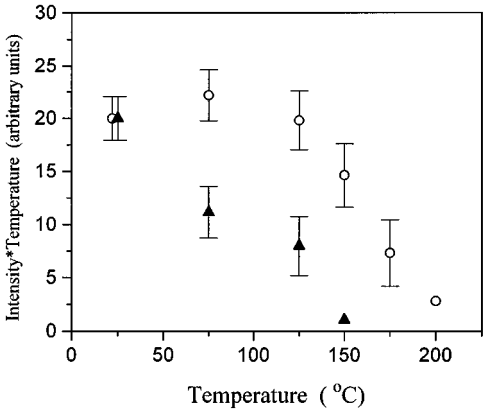

FIG. 4. ^{63}Cu(2) spin-echo intensity at fixed τ values, corrected for Boltzmann factor ($I \times T$), versus temperature. Open circles: sample A; closed triangles: sample B.

Similar losses of NQR intensity were observed in other samples. Taken together, these results show that the onset of anomalous NQR intensity loss occurs at relatively lower temperatures in samples whose room-temperature NQR lines indicate higher defect concentrations. In the most defective material investigated (sample B), the effect is significant even at room temperature.

C. NMR spectra at elevated temperatures

To provide another perspective on the NQR signal loss, we investigated the quadrupolar-perturbed NMR spectrum of $YBa_2Cu_3O_7$ at temperatures above room temperature. Because of the relatively strong electric quadrupole interaction, the ^{63}Cu NMR spectrum in powdered samples of $YBa_2Cu_3O_7$ is severely broadened by the random orientation of powder particles in the external magnetic field. In the 8.0 T magnetic field used in these experiments, the ''central'' ($m = +\frac{1}{2} \leftrightarrow m = -\frac{1}{2}$) transition is broadened to about 5 MHz and quadrupolar-satellite intensity ($m = \pm\frac{1}{2} \leftrightarrow m = \pm\frac{3}{2}$) is distributed from roughly 30 MHz below the central transition to 30 MHz above. Oriented single crystals yield sharp NMR lines but are subject to severe loss of signal intensity due to rf skin depth effects. It has thus become standard practice to use oriented powder samples for NMR studies of $YBa_2Cu_3O_7$ and other high-T_c cuprate superconductors. This technique exploits the highly anisotropic magnetic susceptibility of these materials to orient single-crystal powder particles. When oriented in the normal state, particles align with the CuO_2 planes perpendicular to the external field (''c-axis orientation''). Fixed, oriented arrays can be obtained when the powders are mixed with epoxy resin which is allowed to harden in a high magnetic field. In c-axis orientation, such samples yield a series of relatively narrow lines corresponding to the central and satellite transitions of Cu(1) and Cu(2).

We attempted to prepare an oriented powder sample for NMR at elevated temperatures using a high-temperature epoxy. The spectrum of this sample indicated that a relatively high degree of orientation had been achieved, but there was an unexpected loss of signal intensity at room temperature. Out of concern that there may have occurred a chemical reaction between the sample material and the epoxy which would have been enhanced at elevated temperatures, we elected to work with ''naturally oriented'' loose powders. This procedure, while preserving the chemical integrity of the material at elevated temperatures, limited the measurements to c-axis orientation. As a practical matter, it also required that all measurements on a particular sample be carried out in a single experimental ''run'' since any disturbance of a sample could change the degree of powder orientation.

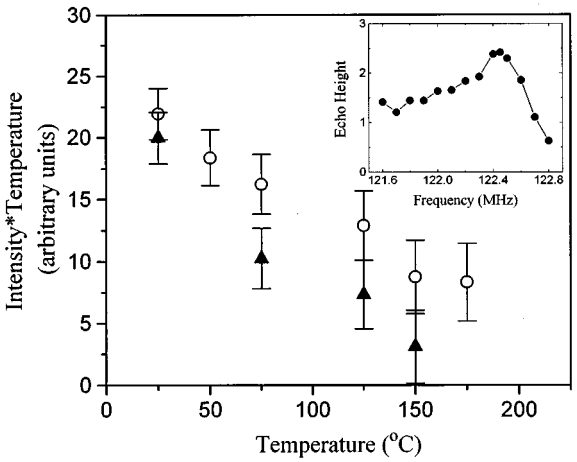

FIG. 5. ^{63}Cu(2) NMR quadrupole-satellite (open circles) and NQR (closed triangles) spin-echo intensities corrected for Boltzmann factor versus temperature for sample C. Inset: ^{63}Cu(2) NMR quadrupole satellite spectrum in partially oriented sample C.

The splitting of the $m = \pm\frac{1}{2} \leftrightarrow m = \pm\frac{3}{2}$ satellite is directly proportional to the electric quadrupole interaction and therefore, as with the NQR frequency, is extremely sensitive to changes in the local electric field gradient. The temperature-corrected Cu(2) satellite intensity is shown as a function of temperature in Fig. 5 and compared with the behavior of the NQR intensity in the same sample. On the basis of its room temperature NQR linewidth, the quality of this sample (C) was intermediate between samples A and B discussed previously. It can be seen that both the NQR and NMR satellite intensities decrease dramatically between room temperature and 450 K. The NMR satellite intensity appeared to survive to slightly higher temperatures than that of the NQR line, but the difference is comparable with the estimated experimental errors. In contrast with the sharp loss of satellite intensity, we observed no appreciable change in the central transition over this temperature range. We attribute this to the fact that the NMR frequencies in the central transition are shifted only in second order by the quadrupole interaction and are thus less sensitive by nearly an order of magnitude to changes in the local electric field gradient.

D. Relaxation effects: Spin-echo damping

The dominant characteristic of the NQR spectra of $YBa_2Cu_3O_7$ samples at elevated temperature is the apparent loss of intensity without appreciable increase in the inhomogeneous linewidth. Since the spin-echo spectra were obtained using a fixed value of the pulse delay τ, this behavior could be explained, at least phenomenologically, by increased damping of the echo during the interval 2τ between

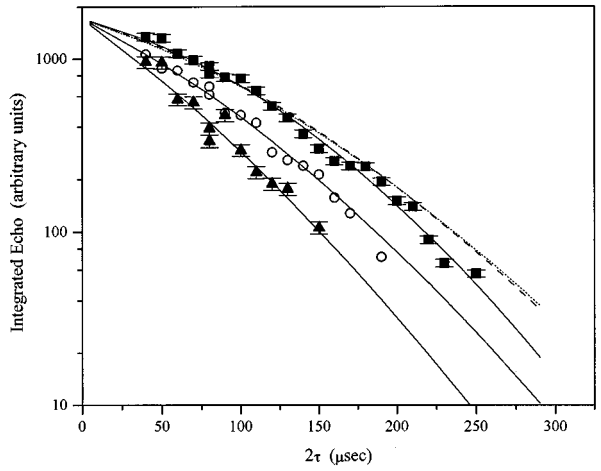

FIG. 6. ^{63}Cu(2) NQR spin-echo decay (integrated intensity versus echo time 2τ) for sample C at 175 K (closed squares), 300 K (open circles), and 350 K (closed triangles). Solid lines are fits using Eq. (1). Dotted and dashed lines represent, respectively, predicted decays at 300 and 350 K taking into consideration only spin-spin and spin-lattice relaxation effects.

the initiating $\pi/2$ rf pulse and the formation of the echo. In general the decay of a spin echo is governed by both simple exponential and Gaussian terms, i.e., the intensity $I(2\tau)$ is given by the relation

$$I(2\tau)=I(0)\exp\left(-\frac{2\tau}{T_{2L}}-\frac{2\tau^2}{T_{2G}^2}\right), \tag{1}$$

where T_{2L} and T_{2G} are, respectively, decay constants related to Lorentzian (exponential) and Gaussian components. The Gaussian constant T_{2G} is normally determined by spin-spin interactions. It has been thoroughly investigated in both NMR and NQR by a number of workers[16–19] because of its dependence on the real part of the nonuniform electronic spin susceptibility. The Lorentzian decay constant is usually dominated by the effect of nuclear spin-lattice relaxation on echo decay. Given independent measurements of the spin-lattice relaxation time T_1, this contribution to T_{2L} can be evaluated according[17] to $1/T_{2L}^{\rm sl}=1.85/T_1$.

The upper curve in Fig. 6 shows a fit of Eq. (1) to the echo decay for sample C at 175 K. The value of the Lorentzian constant was taken from spin-lattice relaxation data in the literature;[11] the Gaussian constant and the absolute intensity $I(0)$ were fitting constants. It was necessary to obtain T_{2G} from a fit to the data since this parameter can depend on the amplitude of the rf pulses in an uncontrolled way. As the echo intensity was not anomalous in this temperature range, i.e., obeyed the Curie law, we believe that the observed decay is completely determined by spin-spin and spin-lattice relaxation effects at this temperature. Our value of T_{2G} at 175 K (120 μs) is within 10% of the value measured at this temperature by Itoh *et al.*[17] indicating that the radio frequency pulse power conditions were quite similar in the two experiments.

To obtain fits to the decays observed at higher temperatures, we assumed that the *temperature dependence* of T_{2G} is comparable with that observed by Itoh *et al.* and extrapolated into the range of higher temperatures explored in our experiments. The temperature dependence of T_{2G} actually becomes very weak near room temperature.[17] We used the spin-lattice relaxation data of Pennington *et al.*[11] to fix $T_{2L}^{\rm sl}$. It can be seen in Fig. 6 that this procedure fails to account for the observed decays in sample C at 300 and 350 K. The predicted decays at these temperatures are, in fact, nearly indistinguishable and slightly slower than the 175 K decay. This simply reflects the relatively weak temperature dependences of the spin-spin and spin-lattice relaxation rates over this temperature range. The essential result of this analysis is that there is a extra component to the spin-echo decay at 300 and 350 K which is not accountable by ordinary relaxation effects. We characterize this extra effect by an additional exponential relaxation component T_{2L}^x. It is the increase of this extra damping that is responsible for the apparent loss of spin-echo intensity at higher temperatures.

Ideally, one would like to repeat the above analysis at a series of temperatures and samples to obtain the dependence of T_{2L}^x on temperature and sample quality. The practicality of this procedure is, however, severely limited by the available signal-to-noise ratios and the nature of the effect. The data indicate that T_{2L}^x becomes progressively shorter at higher temperatures leading to ever more severe spin-echo damping. Thus the observed spin-echo signal at the shortest practical τ values is disappearing just in the range where one would wish to study its decay. On the other hand, at sufficiently low temperatures, T_{2L}^x presumably becomes so long that it cannot effectively compete with ordinary relaxation effects—this is the regime of Curie law behavior for the NQR intensity.

In order to extend the window available for determination of T_{2L}^x, we have adopted the following alternative to direct measurement of the decay curves. Given values of $T_{2L}^{\rm sl}$ and T_{2G} at each temperature determined as discussed above, we determined the value of T_{2L}^x necessary to explain the observed spin-echo intensity at the measurement time of $2\tau=50$ μs. The temperature dependence of $1/T_{2L}^x$ obtained in this way for samples A and C is shown in Fig. 7. These values of $1/T_{2L}^x$ compare well with those obtained directly from the decay curves.

The $1/T_{2L}^x$ data for samples A and B differ significantly. For example, at 425 K, T_{2L}^x is more than ten times shorter for the lower quality sample (C) than for the better sample (A). The latter must be heated to about 475 K to obtain the same value of T_{2L}^x. Also, the onset of extra damping occurs at a higher temperature in sample A, then increases more rapidly than is the case for sample C.

IV. ANALYSIS AND DISCUSSION

The central observation of this investigation is the discovery of an additional damping process for the NQR or NMR satellite spin echo. The excess damping is unrelated to the known spin-spin and spin-lattice relaxation effects and is progressively stronger in more defective samples and at higher temperatures. The damping becomes sufficiently strong that we were unable to observe spin echoes in any sample above 500 K and we are unaware of any such observations in other laboratories. We propose that the extra damping reflects changes in the local electric field gradient

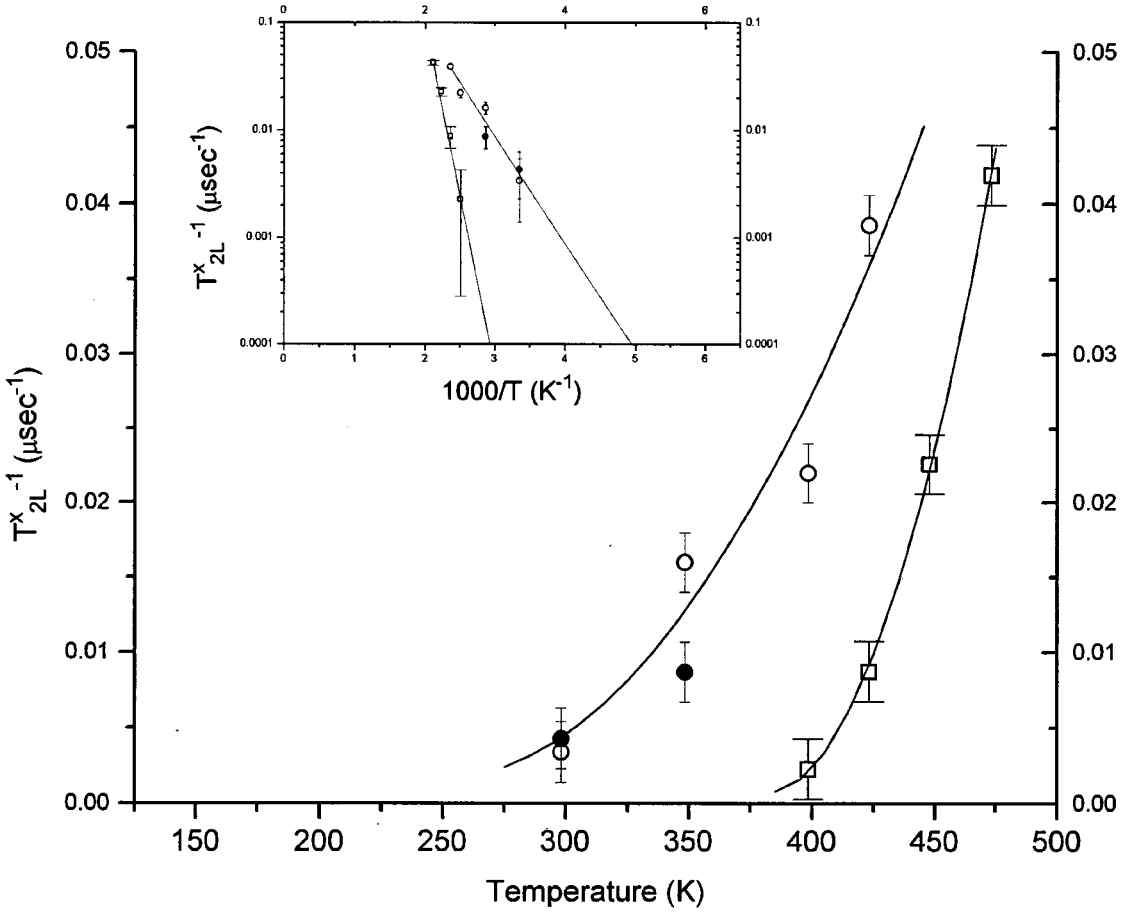

FIG. 7. Extra damping rate $1/T^x_{2L}$ versus temperature for samples A (squares) and C (circles). Closed points (sample C) were obtained by analysis of the NQR spin-echo decay curves of Fig. 6. Open points were determined from relative echo intensity at the measurement value of 2τ (50 μs). Inset: Semilogarithmic plot of the same $1/T^x_{2L}$ data versus inverse temperature.

caused by local atomic motion.

The formation of a spin echo in NQR (or NMR satellite transition) requires ''phase memory,'' that is, individual nuclei must remain in essentially the same local EFG, from the time of the initiating $\pi/2$ pulse until the time of echo formation 2τ. A particular nucleus will not contribute to the spin echo if, during this interval, its quadrupolar frequency changes by more than $\delta\nu_{\rm NQR}\approx 1/\Delta t$, where Δt is the width of the spin echo. For these experiments, $1/\Delta t\approx 200$ kHz. As we discuss in more detail below, short-range motion such as the hop of an oxygen atom into a nearby vacancy almost certainly shifts the quadrupolar frequencies of nearby nuclei by amounts exceeding this limit. Phase coherence will be lost and the spin-echo contributions of these neighbors will be destroyed even if the local environment is restored by a return hop into the oxygen atom's original position unless the total ''round trip'' occurs rapidly compared with the NQR precession period ($1/\nu_{\rm NQR}\approx 32$ ns).[20] The values of T^x_{2L} observed in these experiments, ranging from about 10 μs to 1 ms define the time scale of changes in the local EFG at Cu nuclei for the range of temperatures and defect concentrations investigated. In the following we develop this proposal in more detail by means of an illustrative model and relate the observed damping times to motional times obtained by other experimental techniques.

We begin by mentioning two important observations which reveal the extraordinary sensitivity of NQR to the local environments in a crystalline material. First, it has been the experience of many laboratories that the NQR lines of $YBa_2Cu_3O_7$ are surprisingly broad and variable in samples which are apparently of high quality according to other methods of characterization. These methods include, for example, x-ray diffraction and magnetic examination of the temperature and sharpness of the superconducting transition. Linewidths of 100 to 300 kHz are typically observed for ^{63}Cu(2), whereas the intrinsic linewidth expected from spin-spin interactions in a perfect crystal is on the order of 1 kHz. As discussed previously, Schiefer *et al.*,[14] showed that some of the extra linewidth can be attributed to oxygen deficiency. However, extrapolation of their data to ideal stoichiometry suggested residual linewidths considerably larger than the theoretical estimates. Thus, evidence indicates that even the ''best'' material of nominal composition $YBa_2Cu_3O_7$ probably contains defects and/or lattice strain sufficient to broaden Cu NQR lines to many times their ideal widths. Candidates for the defects responsible of the residual broadening must include oxygen in wrong sites, O(5), and defects on the cation lattice.

The second example of NQR sensitivity is provided by the effect of oxygen deficiency on the Cu(2) NQR spectrum. It is generally accepted that the primary defect associated with small oxygen deficiency is the chain oxygen O(1) va-

cancy. Studies[7,9,10] of material with large deviations from stoichiometry, i.e., material in the range $YBa_2Cu_3O_{6.5}$ to $YBa_2Cu_3O_{6.9}$, show that the various possible arrangements of oxygen in the chain layer, generate a whole new set of Cu(2) NQR lines shifted by as much as several MHz from the nominal $YBa_2Cu_3O_7$ frequency of 31.5 MHz. In effect, the pattern of oxygen arrangements in the CuO chain layer is mapped onto distortions the CuO_2 planes leading to new NQR frequencies for the various distorted Cu(2) sites. These observations lead us to expect an O(1) vacancy to shift the NQR frequency of nearby Cu(2) nuclei in the adjacent planes outside the 200–300 kHz range of observation and to broaden the contributions of more distant Cu(2) sites. The vacancy, of course, has a similar effect on the Cu(1) line—shifting the closest Cu(1) sites far outside the resonance while broadening the observed resonance due to the remaining sites.

Given that oxygen in the CuO chain layer is the most mobile atomic species and that the Cu(2) frequency is highly sensitive to the arrangement of these oxygen atoms, one should expect oxygen motion to attenuate the spin echo, *provided that the motion occurs on an appropriate time scale.* Experimental studies of strain-induced atomic motion (internal friction) by Cost and Stanley[21] suggest that the average atomic hopping rates are relatively slow compared with the time scale of interest in NQR experiments in the same temperature range. For example, the internal friction experiments yield a mean hopping time $\langle \tau \rangle \approx 0.1$ sec at 500 K compared with $T_{2L}^x \approx 10\ \mu$s from NQR (Fig. 7). However, Cost and Stanley also found that their data implied a relatively broad distribution of hopping energy barriers with ''tails'' extending from about 0.8 to 1.5 eV. This is consistent with the relatively high defect concentrations in typical '' $YBa_2Cu_3O_7$.'' Defects can be expected to produce a distribution of energies for occupation of O(1) and O(5) sites[22] as well as a range of energy barriers for hops between these sites. NQR spin-echo damping will be dominated by the most rapid motions associated with the lowest energy barriers.

A detailed and quantitative description of defect-enhanced motion in $YBa_2Cu_3O_7$ lies outside the scope of this paper. We can, however, illustrate how Cu NQR might be affected by motion and estimate the time scale by means of a simple model. Consider an oxygen O(1) vacancy in a CuO chain (Fig. 8). As discussed above, we would expect the frequencies the neighboring Cu(1) nuclei to be shifted far outside the experimental bandwidth. We also expect large shifts of the resonances of the pair of corresponding Cu(2) nuclei, i.e., those connected to the Cu(1) first neighbors by apical oxygens. Assume for simplicity, however, that the resonances of the next most distant Cu(1) sites as well as their connected Cu(2) sites remain within the strain-broadened NQR line. As illustrated in Fig. 8, there are ten such sites in each of the three layers (CuO chain layer and two adjacent CuO_2 planes).

The presence of an O(1) vacancy in the chain lowers the energy for occupation of a neighboring interchain O(5) site[22] and should also lower the barrier for a O(1)→O(5) hop. This is a specific example of the kind of defect-related low-energy hop responsible for the low-energy tail of the barrier distribution. Now the excess damping rate $1/T_{2L}^x$ corresponds to

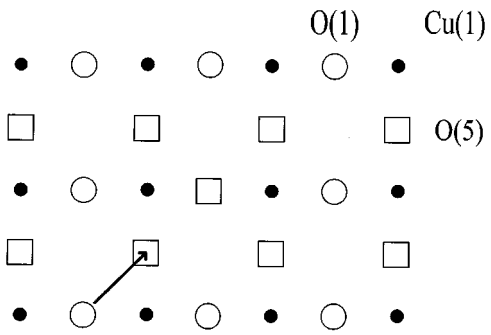

FIG. 8. Portion of CuO chain layer showing Cu(1)-O(1) chains running from left to right. Solid circles denote Cu(1) sites, open circles denote occupied O(1) sites in chains, open squares denote vacant O(5) sites between chains and one vacant O(1) site in center chain. Arrows represents motion of O(1) oxygen atom into O(5) vacancy facilitated by vacancy in neighboring (center) chain.

the probability p that a given Cu(2) will be affected by such a hop. To estimate p, let us assume that the probability p_{15} of an O(1)→O(5) hop is governed by the lowest-energy barriers inferred by Cost and Stanley,[21] i.e., $p_{15} \approx 10^{13} e^{-0.8\ \mathrm{eV/kT}}$. Then, for a given fraction f_1 of vacant O(1) sites, the probability p for elimination of the contribution of a particular Cu(2) to the spin echo will be given by

$$p = 2\, f_1 p_{15}[2(2) + 4(1) + 4(3)], \tag{2}$$

where the terms in the bracket account for each of the ten neighboring Cu sites (Fig. 8) and the multiplicity of O(1)→O(5) hops that could affect the echo contribution of each. For a vacancy concentration $f_1 = 0.02$ and temperature of 500 K, we find $p \approx 8 \times 10^4\ \mathrm{s}^{-1}$. The NQR data imply a value $p = 1/T_{2L}^x \approx 10^5\ \mathrm{s}^{-1}$. Thus, with parameters we consider reasonable, this simple model can account for the magnitude of the observed spin-echo damping.

In the spirit of this model, the effect of increasing defect concentrations can be understood in terms of modification of the barrier distribution. The data show that excess spin-echo damping is enhanced at lower temperatures in more defective samples. Thus, the onset of excess damping occurs at lower temperatures and the temperature dependence is weaker for the lower-quality sample as shown in Fig. 7. This result suggests that the energies of the lowest barriers are reduced further as the defect concentration increases.

The actual situation is undoubtedly much more complex than implied by the simple model we have described. We have, for instance, considered only one specific example of short-range atomic motion. Another possibility is a complementary event in which the presence of an oxygen in an O(5) site could enhance movement of a nearby O(1) oxygen into an unoccupied O(5) site. Such a motion would also disrupt the spin-echo contribution of Cu sites near the new O(5). We also cannot exclude motion enhancement by other defects including disorder on the cation lattice. Finally, we note that it is also likely that these motions influence the Cu EFG over a range beyond the first- and second-neighbor effects assumed here. In this case, a single oxygen hop would affect additional Cu sites and thus attenuate the spin echo more effectively.

A complete description of these processes would also have to include strongly correlated oxygen motions whereby an initiating hop creates a situation in which additional motions are more likely. Consider for example the simple O(1)→O(5) hop of our illustrative model. The new O(1) vacancy created by the hop would lower the barrier for another O(1) to move into an O(5) site near the vacancy. Sequences of such motions together with the restoring O(5)→O(1) hops have been considered as a mechanism for oxygen diffusion.[22] Another example of correlated motion is the rapid motion of oxygen from O(5) to O(5) sites in the interchain channels following an initiating O(1)→O(5) hop. Such defect-enhanced correlations invalidate simple independent-event statistics and thus could contribute to the weaker temperature dependence of T_{2L}^{x} observed in our most defective sample (Fig. 7).

V. SUMMARY

Our analysis of excess NQR and NMR quadrupole satellite spin-echo decay in nominal $YBa_2Cu_3O_7$ between room temperature and 500 K has established the time scale for radical changes in the local EFG at Cu(2). In this interpretation, spin echoes are attenuated because local atomic motion of oxygen in the CuO chain layer destroys coherence in the quadrupolar transition frequency of nearby Cu(1) and Cu(2) nuclei. We observed strong variations from sample to sample in more defective material, the onset of spin-echo attenuation begins at lower temperatures and exhibits a weaker temperature dependence. We attribute this sample dependence to the effect of defects on the distribution of barrier energies for oxygen hops. Enhancement and extension of the low-energy ''tail'' of the barrier distribution would affect the NQR spin echoes most strongly. We have demonstrated the plausibility of this interpretation using a specific model for oxygen hops enhanced by the presence of a nearby vacant O(1) chain site. The illustrative model permits the spin-echo decay times to be rationalized with the seemingly slower time scales of individual oxygen motions inferred by other techniques, especially internal friction. Those studies, in turn, are reasonably consistent with the annealing effects observed at room temperature and below. We emphasize, however, that there are several possible defects that could play a role, including defects on the cation lattice. The model was applied at a temperature of 500 K, where the spin-echo decay times appear to be only weakly dependent on sample quality. The inference is that intrinsic, thermally generated defects dominate at this temperature and above. At lower temperatures, the dependence on defect concentration is strong, implying that a high degree of crystalline perfection is necessary to stabilize the structure of $YBa_2Cu_3O_7$ near room temperature.

*Present address: Doty Scientific, Inc., Columbia, SC 29229.
†Present address: Applied Materials, Sunnyvale, CA 95054.

[1] B. W. Veal *et al.*, Phys. Rev. B **42**, 4770 (1990).
[2] B. W. Veal *et al.*, Phys. Rev. B **42**, 6305 (1990).
[3] J. D. Jorgensen *et al.*, Physica C **167**, 571 (1990).
[4] V. G. Hadjiev *et al.*, Phys. Rev. B **47**, 9148 (1993).
[5] D. de Fontaine, G. Ceder, and M. Astra, Nature (London) **343**, 544 (1990).
[6] J. Zaanen *et al.*, Phys. Rev. Lett. **60**, 2685 (1988).
[7] W. W. Warren, Jr. *et al.*, Phys. Rev. B **39**, 831 (1989).
[8] G. Ceder, R. McCormack, and D. de Fontaine, Phys. Rev. B **44**, 2377 (1991).
[9] H. Yasuoka, T. Imai, and T. Shimizu, in *Strong Correlation and Superconductivity*, edited by H. Fukuyama, S. Maekawa, and A. P. Malozemoff (Springer, Berlin, 1988).
[10] A. J. Vega *et al.*, Phys. Rev. B **39**, 2322 (1989).
[11] ^{63}Cu spin-lattice relaxation times were measured up to 500 K by C. H. Pennington *et al.*, quoted by C. H. Pennington and C. P. Slichter, in *Physical Properties of High Temperature Superconductors II*, edited by D. M. Ginsberg (World Scientific, Singapore, 1990).
[12] M. Bankay *et al.*, Phys. Rev. B **46**, 11 228 (1992).
[13] Susan P. Klein, Ph.D. Thesis, Oregon State University, 1995.
[14] H. Schiefer *et al.*, Physica C **162-164**, 171 (1989).
[15] D. Brinkmann, Physica C **153-155**, 75 (1988).
[16] C. H. Pennington and C. P. Slichter, Phys. Rev. Lett. **66**, 381 (1991).
[17] Y. Itoh *et al.*, J. Phys. Soc. Jpn. **61**, 1287 (1992).
[18] T. Imai *et al.*, Phys. Rev. B **47**, 9158 (1993).
[19] M. Takigawa, Phys. Rev. B **49**, 4158 (1994).
[20] We wish to make clear that the variations of the local electric field gradient considered here are far too slow to be effective in the context of conventional motional narrowing theory. Thus there is no narrowing of the inhomogeneously broadened NQR line as the temperature is raised. The proposed mechanism is based on a strong-scattering ''collision'' model in which a single event suffices to eliminate the spin-echo contributions of a small number of affected nuclei. At some temperature sufficiently high that all nuclei ''see'' essentially the same time-averaged electric field gradient, the motionally narrowed NQR line should, at least in principle, reappear.
[21] J. R. Cost and J. T. Stanley, J. Mater. Res. **6**, 232 (1991).
[22] J. R. LaGraff and David A. Payne, Physica C **212**, 487 (1993).